

Surface activated carbon nanospheres for fast adsorption of silver ions from aqueous solutions

Xianghua Song, Poernomo Gunawan, Rongrong Jiang, Susanna Su Jan Leong, Kean Wang, Rong Xu*

School of Chemical and Biomedical Engineering, Nanyang Technological University, 62 Nanyang Drive, Singapore 637459, Singapore

ARTICLE INFO

Article history:

Received 4 May 2011

Received in revised form 21 July 2011

Accepted 22 July 2011

Available online 5 August 2011

Keywords:

Carbon nanosphere

Silver

Adsorption

Sodium hydroxide

Surface activation

ABSTRACT

We report the synthesis and activation of colloidal carbon nanospheres (CNS) for adsorption of Ag(I) ions from aqueous solutions. CNS (400–500 nm in diameter) was synthesized via simple hydrothermal treatment of glucose solution. The surface of nonporous CNS after being activated by NaOH was enriched with –OH and –COO[–] functional groups. Despite the low surface area (<15 m²/g), the activated CNS exhibited a high adsorption capacity of 152 mg silver/g. Under batch conditions, all Ag(I) ions can be completely adsorbed in less than 6 min with the initial Ag(I) concentrations lower than 2 ppm. This can be attributed to the minimum mass transfer resistance as Ag(I) ions were all deposited and reduced as Ag⁰ nanoparticles on the external surface of CNS. The kinetic data can be well fitted to the pseudo-second-order kinetics model. The adsorbed silver can be easily recovered by dilute acid solutions and the CNS can be reactivated by the same treatment with NaOH solution. The excellent adsorption performance and reusability have also been demonstrated in a continuous mode. The NaOH activated CNS reported here could represent a new type of low-cost and efficient adsorbent nanomaterials for removal of trace Ag(I) ions for drinking water production.

© 2011 Elsevier B.V. All rights reserved.

1. Introduction

Silver as one of the precious metals is in high demand since it plays important roles in many aspects of human life. For example, silver and its compounds are often used as disinfectants in wastewater treatment, food/beverages/drugs processing, and drugs, etc. [1]. On the other hand, the monovalent ionic silver, Ag(I), is of particular environmental concern, due to its potential impact on human health and ecosystems. It has been reported that when ingested by humans, silver is metabolized and deposited in the subcutaneous fat. The greyish-blue color of silver gives rise to the cosmetic disorder of argyria, in which the affected person's skin is discolored [2]. It was also found that ion regulatory failure of the human body due to an inhibition of uptake of active Na⁺ and Cl[–] can be caused by Ag(I) exposure. The World Health Organization (WHO) and the US Environmental Protection Agency (EPA) classified soluble silver ions as hazardous substances in water systems and limited the level of silver in drinking water to be 100 ppb (100 µg/L) [3]. Therefore, with the increasing concerns on the toxicity of soluble silver ions in water and the scarcity of silver sources, it is necessary to remove and recover silver from water. In particular, it remains a challenging task to recover silver from wastewater of low silver concentrations efficiently and economically.

Adsorption has been widely used as an effective separation technology in water treatment owing to its simplicity in process design and operation [4]. Activated carbons are currently the most commercially used adsorbents in treating pollutants in aqueous solutions [5]. The further development of low cost and environmental benign adsorbents is of paramount importance for practical applications [6,7]. In particular, low cost adsorbent materials with fast kinetics and high adsorption capacity for heavy metals like silver ions are expected to be in high demand.

Recently, a “green” synthesis approach has been developed involving transformation of readily available precursors, such as sugars (glucose) [8–10] and cyclodextrins [11] to carbon spheres under mild conditions (hydrothermal reaction at 160–180 °C). The advantage of this synthetic approach is obvious because neither toxic reagents, organic solvents and other additives nor complicated procedures are involved. The surface of the resulting carbon spheres contains rich hydrophilic functional groups such as C–OH, C=O and C–OOH. Up to date, the carbon spheres have been mainly utilized as support materials to deposit metal/metal oxide nanoparticles [9,10,12], and template to synthesis hollow metal/metal oxide nanospheres [13,14]. There have been only a few studies on exploration of carbon spheres in water treatment [15,16]. It is expected that because of the surface active functional groups, the carbon spheres could present promising adsorption performance towards metal ions.

The surface composition and property of the adsorbent materials can be modulated by chemical treatment using various reagents

* Corresponding author. Tel.: +65 6790 6713; fax: +65 6794 7553.
E-mail address: rxu@ntu.edu.sg (R. Xu).

such as acids, bases, oxidants, polymers, etc. [17–20]. For activated carbon and other types of carbon materials, it has been widely reported that the adsorption capacities towards metal ions can be enhanced by chemical treatment with acids and bases [17,18,21–24]. Although the surface of native carbon spheres already contains C–OH and C=O groups, the density of such functional groups can be increased by similar treatment in acids or bases to improve the adsorption properties. To the best of our knowledge, there is no literature reporting the post treatment of carbon spheres by acids and bases for adsorption applications, although carboxylate-rich carbon spheres were prepared by adding acrylic acid monomer during the synthesis of carbon spheres [15].

Herein, the potential application of carbon spheres in removal and recovery of Ag(I) ions from water, especially from water with dilute Ag(I) ion concentrations (<1 ppm) was explored. Colloidal carbon nanospheres (400–500 nm in diameter) were synthesized and activated by a simple treatment with aqueous solutions of NaOH. The effect of alkaline treatment on the surface functional groups and adsorption properties of carbon nanospheres was systematically investigated in batch studies. In addition, a fixed-bed adsorption column was used to investigate the efficiency of Ag(I) ion removal and recovery under the continuous operational mode for potential large-scale applications.

2. Experimental

2.1. Preparation of native carbon nanospheres (CNS)

The fabrication method of the native CNS was based on that reported in the literature [9]. Briefly, 40 mL of an aqueous solution of 0.5 M glucose (α -D(+)-glucose, Acros Organics, 99+, anhydrous) was first ultrasonicated for 30 min. The solution was added into a Teflon-lined autoclave (maximum capacity: 45 mL) which was then subjected to heating at 160 °C for 12 h. The as-prepared colloidal carbon nanospheres were washed with deionized water and ethanol for three times each via centrifugation, then dried in an oven at 60 °C for 12 h.

2.2. Activation of CNS with aqueous solutions of NaOH

To activate the surface of CNS for Ag(I) ion removal, the as-prepared CNS were soaked in the aqueous solutions of sodium hydroxide. Briefly, 0.12 g of dry powder was dispersed in 100 mL of NaOH (Fisher Scientific, 98.95%) aqueous solution of a certain concentration. The mixture was stirred at 300 rpm for 1 h at room temperature. The product was collected by filtration and washed with a copious amount of deionized water (about 1 L) to remove the residual NaOH until the pH of the filtrate reached near neutral. The activated CNS samples were dried in an oven at 60 °C for 12 h. The effect of NaOH concentration was studied. The CNS samples activated with 0.01 M, 0.05 M, 0.1 M, 0.5 M and 1.0 M of NaOH solutions were denoted as CNS/OH0.01, CNS/OH0.05, CNS/OH0.1, CNS/OH0.5 and CNS/OH1.0, respectively. The native sample without activation was named as CNS.

2.3. Materials characterization

The surface functional groups of the samples was analyzed using Fourier transmission infrared spectroscopy (FTIR, Spectrum 1, Perkin-Elmer) using a standard KBr disk technique. The powder X-ray diffraction (XRD) patterns were recorded on a Bruker AXS D8 X-ray diffractometer with Cu K α ($\lambda = 1.5406 \text{ \AA}$) radiation at 40 kV and 20 mA. The morphology was obtained using field emission scanning electron microscopy (FESEM, JEOL 6700F), transmission electron microscopy (TEM) and high resolution TEM (HRTEM) on a

JEOL 3010. The surface area and pore volume were obtained from the adsorption isotherms of nitrogen at $-196 \text{ }^\circ\text{C}$ in a Quantachrome Autosorb-6B apparatus. Zeta potential of the samples in deionized water was determined using a zeta meter (BIC PALS zeta potential Analyser) by dispersing 12.5 mg of the samples in 25 mL of deionized water.

2.4. Adsorption capacities

The adsorption capacities of both native and activated carbon nanospheres were studied in a batch mode. Freshly prepared Ag(I) aqueous solutions (25 mL) from AgNO₃ (Sigma Aldrich, 99+%) with their concentrations ranged 7–320 ppm (ppm: mg silver/L) were dispensed into conical flasks, which contained accurately weighed 25 mg of carbon nanosphere samples. The mixtures were shaken at 200 rpm at room temperature for 12 h. The solutions were then withdrawn and filtered through PTFE syringe filters (pore size: 0.45 μm). The clear filtrates obtained were diluted in 2% HNO₃ for determination of Ag(I) concentration by inductively coupled plasma atomic emission spectroscopy (ICP-AES, Perkin Elmer ICP Optima 2000DV). Prior to this, the effect of the PTFE filter on the measured Ag(I) concentration was found negligible by comparing the concentration difference with and without filtration using the standard Ag(I) solutions in the range of 20 ppb to 100 ppm.

2.5. Adsorption kinetics and mechanism

The adsorption kinetics of Ag(I) with CNS/OH0.5 was carried out at various initial Ag(I) concentrations (98 ppb, 952 ppb, 1.94 ppm and 202 ppm). Briefly, 240 mg of CNS/OH0.5 powder was dispersed in 240 mL of Ag(I) solution and the mixture was stirred at 200 rpm at room temperature. At different time interval, 5 mL of the solution was withdrawn, filtered and diluted in 2% HNO₃ for ICP-AES measurement. The adsorption mechanism of Ag(I) ions on activated carbon nanospheres was investigated by mixing 25 mg of CNS/OH0.5 in 25 mL of 0.01 M (1080 ppm) Ag(I) aqueous solution. The mixture was shaken at 200 rpm for 6 h. The solids after adsorption of Ag(I) ions were collected by centrifugation and dried in oven at 60 °C before characterization by XRD and TEM methods.

2.6. Recovery and reusability

To recover the adsorbed silver and reuse the carbon nanospheres after adsorption, aqueous solutions of 0.2 M and 1.0 M HNO₃ were used to dissolve silver from the surface of carbon nanospheres. The adsorption was first conducted by adding 15 mg of CNS/OH0.5 in 25 mL of Ag(I) solution of 2 ppm. The mixture was shaken at 200 rpm at room temperature for 12 h. The resulting silver adsorbed carbon nanospheres were separated from the solution by centrifugation and dispersed in 25 mL of HNO₃ solution for desorption. The mixture was then shaken at 200 rpm. After a certain period of time, 10 mL of the solution was withdrawn and filtered to get clear solution for ICP-AES analysis. After recovery of silver, the carbon nanospheres were regenerated by soaking in 50 mL of 0.5 M NaOH solution for 1 h at room temperature, followed by washing with deionized water until the pH of the filtrate reached near neutral. The adsorption capacity of the regenerated CNS/OH0.5 was obtained under the same conditions as those used for the fresh CNS/OH0.5 for comparison.

2.7. Continuous study using a fixed-bed adsorption column

The efficiency of sample CNS/OH0.5 in removing Ag(I) ions from solutions of low concentrations (100 ppb and 1 ppm) was studied in a fixed-bed packed column with a filter layer at both ends to

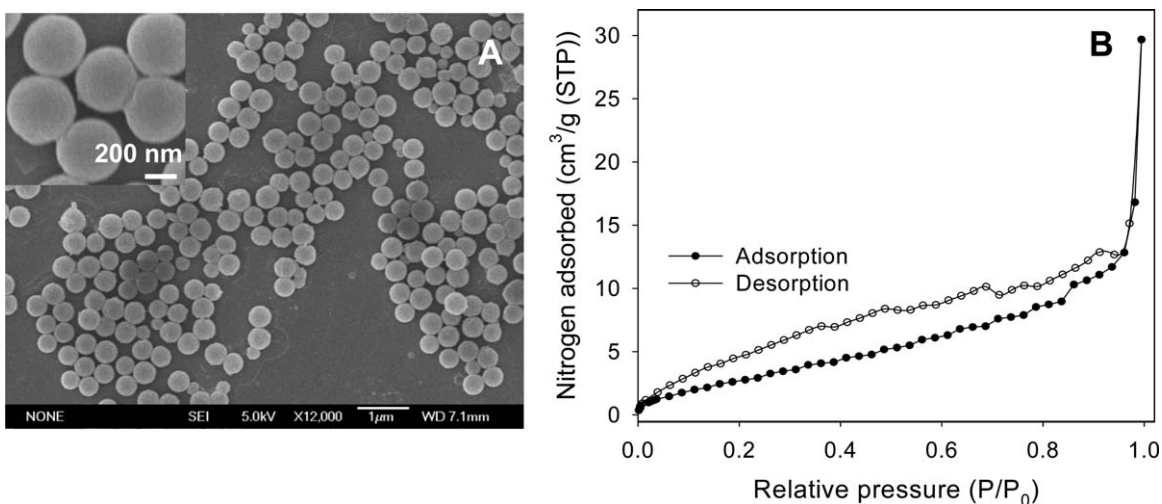


Fig. 1. (A) FESEM image of as-prepared carbon nanospheres (CNS) and (B) N_2 adsorption–desorption isotherm of CNS.

prevent the entrainment of particles by water flow. To avoid excessive pressure drop, CNS/OH0.5 powder was mixed well with silica beads (Acros Organics, particle size: 0.2–0.5 mm) at a mass ratio of 1:50 before packing the column. The inner diameter and length of the column were 1.5 cm and 20 cm, respectively. The amount of CNS/OH0.5 required to fully pack the column was around 240 mg. The continuous adsorption study was carried out at room temperature, during which the Ag(I) solution was fed into the vertically oriented column by a peristaltic pump. The flow mode was downward and the flow rate was fixed at 6 mL/min. At certain time interval, 15 mL of the effluent was collected and diluted in 2% HNO_3 solution for ICP-AES analysis. Breakthrough and exhaustion in continuous adsorption were usually defined as the phenomenon when the concentration of the adsorbate in the effluent reached about 3–5% and 90% of that in the feed, respectively [25]. After saturation was reached, the column was eluted with an aqueous solution of 0.5 M HNO_3 at 5 mL/min with an upward flow mode in the initial 15 min followed a downward flow mode for another 2 h in order to keep the distribution of CNS/OH0.5 particles more evenly distributed in the column. Then column was then washed with deionized water at 5 mL/min for 3 h followed by regeneration with 0.01 M NaOH solution at 5 mL/min for 3 h. Finally, the column was washed with deionized water overnight at 2 mL/min until pH of the effluent water reached around 8.5–9.0. The adsorption performance of the regenerated column was evaluated under the same conditions as those of the fresh column.

3. Results and discussions

3.1. Properties of activated carbon nanospheres

Fig. 1A displays the FESEM image of the as-prepared CNS sample. Well dispersed nanospheres with relatively uniform diameters of around 400–500 nm were formed. Similar to the literature results [8–10], the hydrothermally formed CNS in this work has a non-porous structure as indicated by its low specific surface area of $12.7 \text{ m}^2/\text{g}$. The N_2 adsorption–desorption isotherm shown in Fig. 1B consistently indicates a Type II isotherm typically for non-porous materials [26]. The measured pore volume was as low as 0.02 mL/g which should be mainly contributed by the inter-particle space. Activation of CNS by NaOH of all the concentrations used (0.01–1.0 M) did not cause any noticeable changes in the morphology, surface area and pore volume. Hence NaOH activation only modified the surface of CNS without affecting the bulk carbon core.

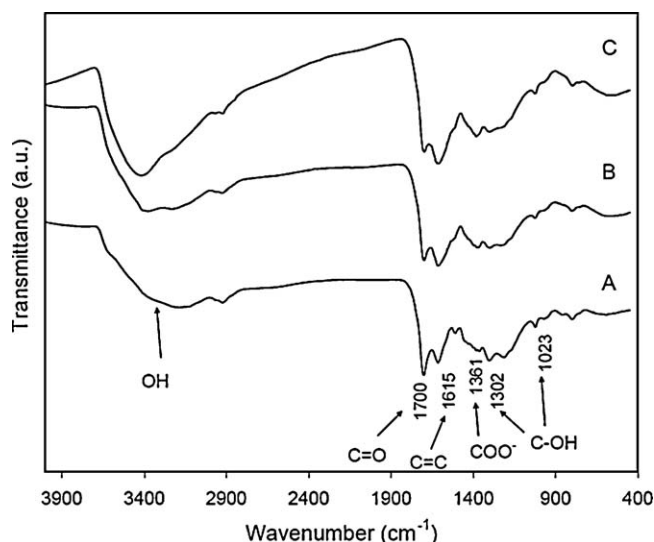
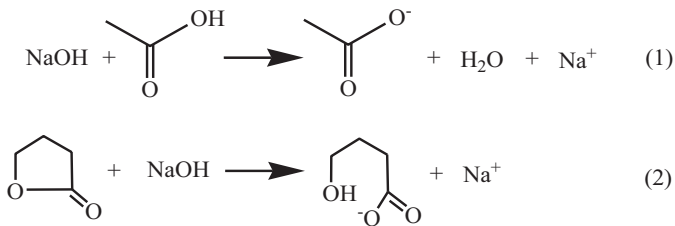


Fig. 2. FTIR spectra of (A) CNS, (B) CNS/OH0.1, and (C) CNS/OH0.5.

The FTIR spectra of CNS, CNS/OH0.1 and CNS/OH0.5 are shown in Fig. 2. The main characteristic absorption peaks of CNS can be assigned accordingly as shown in Fig. 2A: $3100\text{--}3400 \text{ cm}^{-1}$ to O–H stretching vibration, 1700 cm^{-1} to the stretching vibration of C=O in carboxyl group [15,27–30] or lactone group [31], 1615 cm^{-1} to C=C stretching, 2923 cm^{-1} to aliphatic hydrocarbon–CH, 1023 cm^{-1} and 1302 cm^{-1} to C–OH stretching and OH bending vibrations in C–OH, respectively [9,15], and 1361 cm^{-1} to symmetric stretching vibration of deprotonated carboxyl group, $-\text{COO}^-$ [9,32,33]. FTIR spectra of CNS/OH0.1 and CNS/OH0.5 are shown in Fig. 2B and C, respectively. In comparison with that of CNS, the intensity of absorption band in the range of $3100\text{--}3400 \text{ cm}^{-1}$ was significantly increased especially for CNS/OH0.5, which indicates an enrichment of hydroxyl groups after NaOH activation. The deprotonated carboxylate groups ($-\text{COO}^-$) centered at around 1360 cm^{-1} was also noticeably increased [32,33]. Correspondingly, the peak due to C=O stretching in carboxyl and lactone groups at 1700 cm^{-1} was greatly decreased. The above observations suggested that NaOH reacted with the carboxyl and lactone groups present on the surface of CNS according to the following reactions [21,24,34].



Zeta potential of CNS and CNS/OH0.5 dispersed in deionized water was measured to be -28.7 mV and -42.7 mV, respectively. The more negative zeta potential of NaOH activated carbon nanospheres can be consistently interpreted by the occurrence of the above two reactions which generated the negatively charged $-\text{COO}^-$ functional group on the surface [35,36]. The increase in surface densities of the functional groups like $-\text{OH}$ and $-\text{COO}^-$ is expected to be beneficial for adsorption of $\text{Ag}(\text{I})$ ions from water.

3.2. Adsorption capacities

The effect of NaOH concentration for activation of CNS on their adsorption capacities is shown in Fig. 3. At a lower initial $\text{Ag}(\text{I})$ concentration (C_0) of 9 or 38 ppm, the adsorption capacities of various CNS/OH samples were similar. At higher C_0 of 96 ppm, the adsorption capacity was in the order of $\text{CNS}/\text{OH}1.0 \approx \text{CNS}/\text{OH}0.5 > \text{CNS}/\text{OH}0.1 \approx \text{CNS}/\text{OH}0.05 > \text{CNS}/\text{OH}0.01$. It can be seen that the adsorption capacity of sample CNS at higher C_0 was much lower than those of activated carbon nanospheres even when the concentration of NaOH was as low as 0.01 M. The richer surface hydroxyl and deprotonated carboxylic groups on CNS/OH as evidenced in FTIR spectra contributed to the higher adsorption capacities.

The maximum adsorption capacity of CNS/OH0.5 was obtained from the adsorption isotherm with C_0 ranged from 7 ppm to 320 ppm at room temperature (Fig. 4). At relatively lower C_0 of 7 ppm and 40 ppm, C_e measured was almost zero, indicating its high efficiency (>99.9%) in removal of $\text{Ag}(\text{I})$ ions from solutions of low concentrations. The removal percentage at C_0 of 100 ppm was still as high as 98.3%. The maximum adsorption capacity was around 152.1 mg/g when C_0 reached 320 ppm. Although the adsorption capacity of our sample is lower than those of polymeric adsorbents, e.g., poly(aniline-co-5-sulfo-2-anisidine), with functional groups in every unit of the polymer chains [37–40], the NaOH activated CNS obtained in this work is much more efficient than those traditional

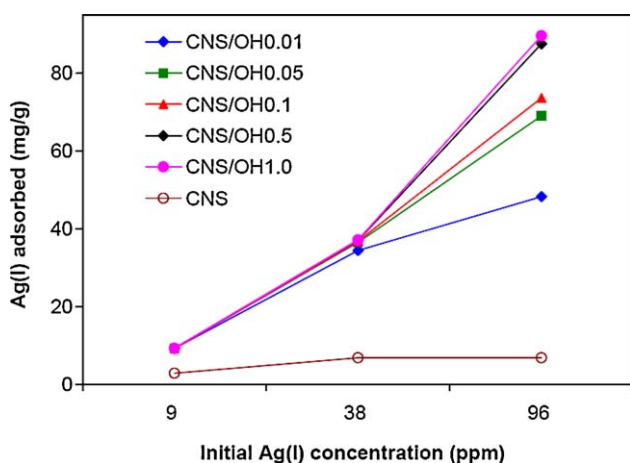


Fig. 3. The effect of NaOH concentration for activation of CNS on their adsorption capacities for $\text{Ag}(\text{I})$ ions.

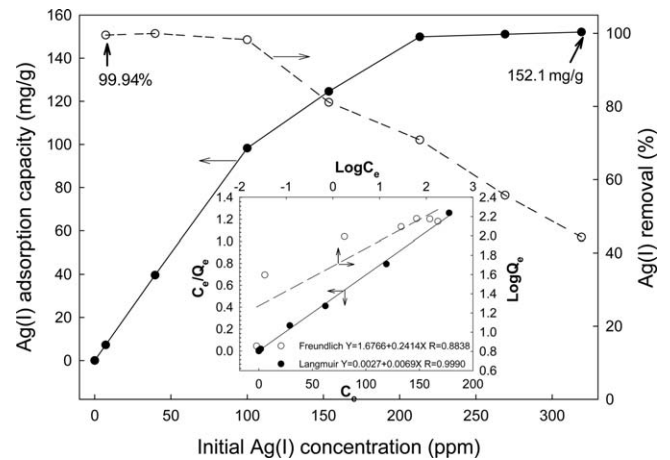


Fig. 4. The adsorption isotherm and the corresponding $\text{Ag}(\text{I})$ ion removal efficiency of CNS/OH0.5; inset: fittings to linearized Langmuir and Freundlich adsorption models.

adsorbents such as activated carbon, coke [41], brewery waste biomass [42], peat [41], etc. Linearized Langmuir and Freundlich adsorption models were used to analyze the adsorption equilibrium of $\text{Ag}(\text{I})$ on CNS/OH0.5. As shown in Fig. 4 inset, Langmuir model can well describe the adsorption of $\text{Ag}(\text{I})$ on CNS/OH0.5 with a correlation coefficient of 0.9990, whereas Freundlich model is not suitable as a low correlation coefficient of 0.8838 was resulted. Langmuir isotherm is based on the assumption of a monolayer adsorption on a homogeneous surface. It can be generally applied to chemisorption and with some restrictions to physical adsorption [43]. The good fitting of our equilibrium data to Langmuir isotherm may indicate the chemisorption mechanism of $\text{Ag}(\text{I})$ onto CNS/OH in aqueous solutions. The maximum adsorption capacity obtained from Langmuir model, Q_m , is 144.9 mg/g, which is very close to the maximum experimental adsorption capacity of 152.1 mg/g. In contrast, the native CNS offered a much lower maximum adsorption capacity of less than 20 mg/g under the same experimental adsorption conditions. Furthermore, the adsorption equilibrium data of native CNS can neither be fitted to Langmuir nor Freundlich model (data not shown).

3.3. Adsorption kinetics and mechanism

The adsorption of metal ions on materials surface can generally be classified to three processes: physical adsorption, ion exchange and complex/redox adsorption. Physical adsorption occurs through the weak van der Waals interaction and hence is not stable. Adsorption via ion exchange is mainly through the exchange of metal ions with the active protons in the adsorbent. The complex/redox adsorption has been often reported when the adsorbents were polymers containing functional groups such as $-\text{NH}_2$, $-\text{CN}$, $-\text{SH}$, $-\text{SO}_3\text{H}$, etc. Such groups have strong chelating ability with metal cations [37,39,40]. Furthermore, if the metal ions belong to the heavy metal group like Ag^+ with a high standard reduction potential, the functional groups are capable to reduce them to metals [37]. Although less well studied, $-\text{OH}$ and $-\text{COOH}$ groups have also been reported capable of reducing Ag^+ to metallic silver [44,45].

To investigate the mechanism of adsorption, adsorption rate was studied and kinetics models were used to describe the adsorption process. As shown in Fig. 5, it was remarkable that $\text{Ag}(\text{I})$ sorption onto the CNS/OH0.5 was very fast at a wide range of C_0 from trace 98 ppb to 202 ppm. The adsorption was completed in less than 6 min with 100% of removal efficiency when C_0 was lower than

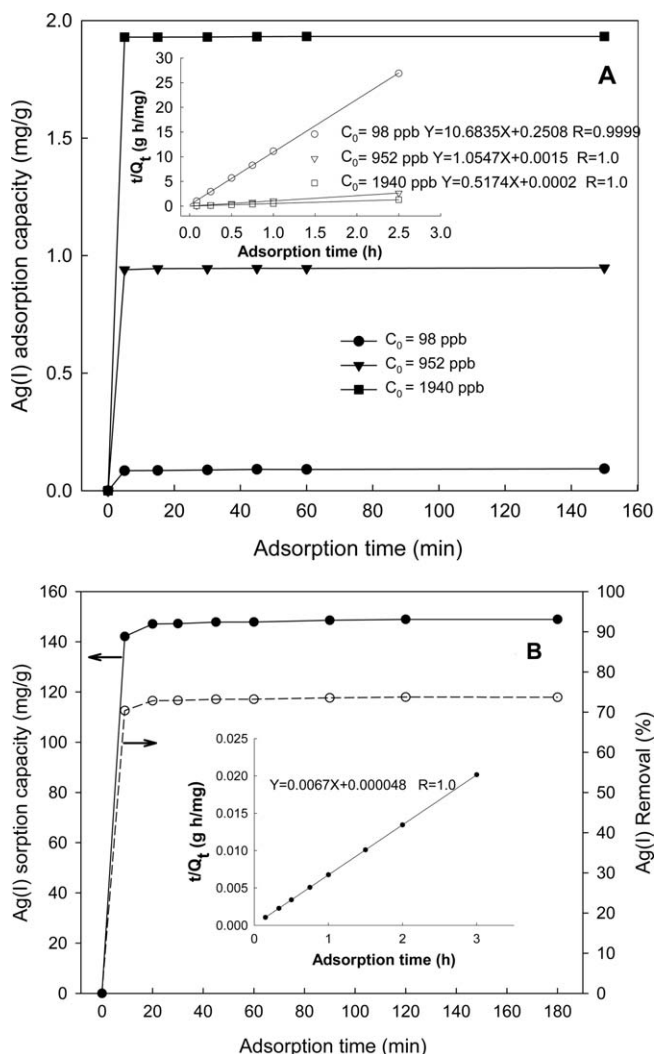


Fig. 5. The amount of Ag(I) ions adsorbed on CNS/OH0.5 at different time, (A) $C_0 = 98$ ppb, 952 ppb and 1940 ppb and (B) $C_0 = 202$ ppm; inset: fittings to the second order kinetics model.

2 ppm (Fig. 5A). With a much higher C_0 of 202 ppm, the adsorption was also completed within a short duration of 20 min and the corresponding removal efficiency was 74% (Fig. 5B). Such fast adsorption kinetics should be attributed to the nonporous structure of the carbon nanospheres. The adsorption mainly took place on the external surface of the colloidal nanospheres with minimum mass transfer resistance. In addition, the surface of our carbon nanospheres was enriched with the functional groups for catching the Ag(I) ions efficiently from even dilute solutions. In contrast, other adsorbents with micro- or mesoporous structures like polymer, activated carbon, chitosan, etc., often take long time (typically a few hours to days) to reach the adsorption equilibrium [37,39–42,46]. Our Ag(I) sorption kinetic data can be well fitted to the pseudo-second-order kinetics model with almost perfect correlation coefficient of 0.9999–1.0 (Fig. 5 inset), while poor fittings were generated if the pseudo-first-order model was used (results not shown). As the pseudo-second-order model is based on the assumption that chemical sorption is the rate-determining step [42], the above results obtained consistently suggested that the Ag(I) ions were chemically adsorbed.

To provide further evidences for the redox adsorption mechanism, CNS/OH0.5 after adsorption of Ag(I) ions from the solution with a high C_0 of 1080 ppm (0.01 M) was analyzed with XRD and TEM techniques. The XRD pattern of this sample (Fig. 6A-a) can be indexed to face-centered cubic (FCC) metallic Ag⁰ crystals (PDF no. 001-1167) as indicated by the presence of (1 1 1), (2 0 0) and (2 2 0) planes. The XRD pattern of CNS/OH0.5 before Ag(I) adsorption (Fig. 6A-b) only exhibits a broad and weak band at around 20° which can be assigned to the amorphous phase of CNS [47]. The TEM image (Fig. 6B inset) indicated that nanoparticles of around 5–30 nm were deposited on the surface of carbon nanospheres. The high resolution TEM image of an individual nanoparticle (Fig. 6B) shows a lattice distance of 0.224 nm which is in good agreement with that of the (1 1 1) plane of FCC metallic Ag⁰. The above results provide direct evidences for the redox adsorption of Ag(I) ions to Ag⁰ nanoparticles on NaOH activated carbon nanospheres due to their rich surface functional groups of –COO[–] and –CH₂OH groups. The chelating ability of carboxylate group towards heavy metals ions like Ag(I) has been reported [48–50]. On the other hand, it has been shown that the hydroxyl group of poly(ethylene glycol) can reduce Ag(I) to Ag⁰ accompanied by oxidation of hydroxyl to aldehyde group [44]. Hence the chelation/redox mechanism in which

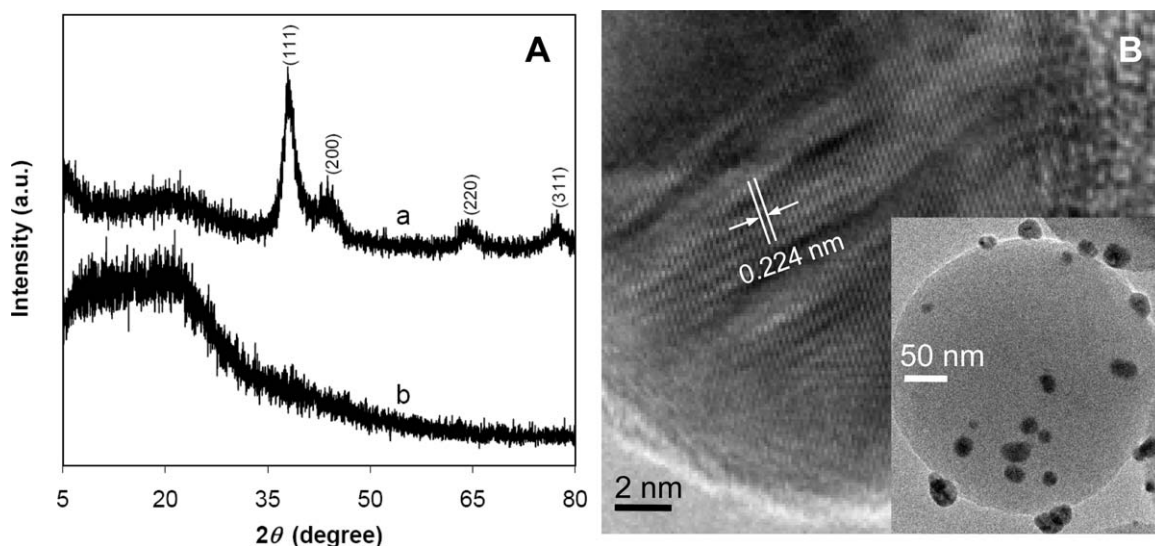


Fig. 6. (A) XRD patterns of CNS/OH0.5 (curve a) and CNS/OH0.5 after adsorption of Ag(I) ions (curve b) and (B) HRTEM image of a representative silver nanoparticle formed on CNS/OH0.5 after adsorption of Ag(I) ions; inset: TEM image of the same sample.

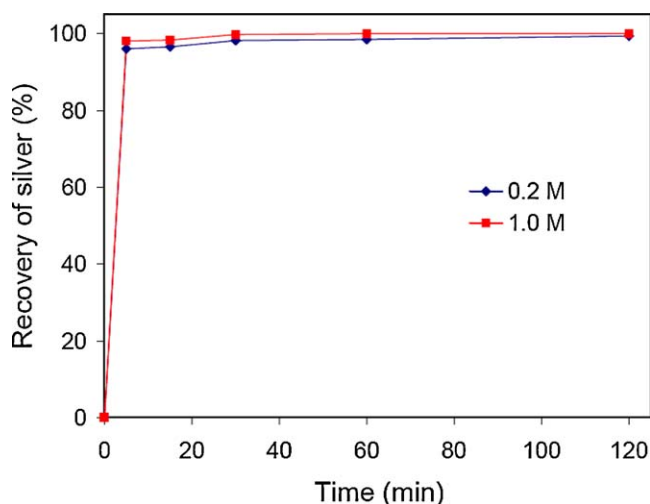
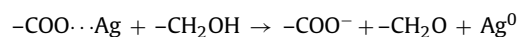
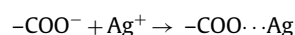


Fig. 7. The percentage recovery of Ag(I) ions from CNS/OH0.5 adsorbed with Ag(I) ions with aqueous solutions of HNO₃ at 0.2 M and 1.0 M.

–COO[−] acts as a chelating group and –CH₂OH acts as a reducing agent is proposed for our process.



3.4. Recovery of silver after adsorption and regeneration of CNS/OH0.5

Aqueous solutions of HNO₃ were used to recover silver from CNS/OH0.5 after adsorption with C₀ at 1920 ppb. The eluted Ag(I) ion concentration and recovery percentage at different time duration are shown in Fig. 7. It can be seen that desorption (or rather dissolution) was also very fast since silver nanoparticles were only present on the external surface of carbon nanospheres. More than 96% and 99% of Ag(I) can be recovered in 5 min and 2 h, respectively, even when a lower HNO₃ concentration of 0.2 M was used. After desorption of Ag(I) ions in the acidic solution, the carbon nanospheres were reactivated with 0.5 M NaOH. The adsorption capacity of the regenerated CNS/OH0.5 sample was almost the same as that of the original CNS/OH0.5. Hence it was demonstrated that the functional groups for Ag(I) adsorption can be easily regenerated by treatment with NaOH again.

3.5. Removal of Ag(I) ions in a continuous mode

Owing to the fast adsorption rate, the activated carbon nanospheres could be potentially used in a continuous mode for large-scale applications. The removal of Ag(I) ions (C₀ at 1 ppm) in a continuous mode with CNS/OH0.5 packed in a fixed-bed column was studied. The breakthrough curves, i.e., the plot of the effluent Ag(I) concentration versus the contact time, are shown in Fig. 8. The column can remove almost all Ag(I) ions with the effluent Ag(I) concentrations lower than 10 ppb in the initial 35 h. After saturation, the column was regenerated in the same column and reused for adsorption. The regenerated column exhibited the similar adsorption performance for Ag(I) removal with the breakthrough time slightly reduced to 32 h. In addition, the removal of the trace amount of Ag(I) ions (C₀ at 100 ppb) with the packed column was studied. The curve in Fig. 8 shows that the effluent Ag(I) concentration reached breakthrough point only after 46 h. Thus the NaOH activated carbon nanospheres developed in this work could be potentially applied for large-scale water treatment.

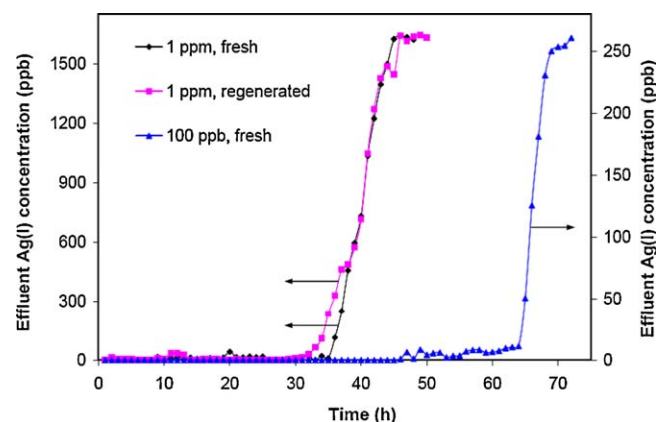


Fig. 8. The effluent Ag(I) concentration versus the contact time in a continuous mode using a fixed-bed packed with a mixture of CNS/OH0.5 and silica beads, C₀ = 1 ppm (fresh and regenerated column) and 100 ppb (fresh column).

4. Conclusions

Colloidal carbon nanospheres (CNS) obtained by a “green” synthesis method can be easily activated with aqueous solutions of NaOH. The surface of the activated carbon nanospheres was enriched with functional groups of –COO[−] and –OH which induced chelation and redox adsorption of Ag(I) ions to metallic silver nanoparticles. The maximum adsorption capacity obtained with carbon nanospheres activated with 0.5 M NaOH was 152 mg/g. With the initial Ag(I) concentration lower than 2 ppm and the adsorbent dosage of 1 g/L, all Ag(I) ions can be adsorbed within the first 6 min. Such fast adsorption kinetics can be attributed to the nonporous structure and rich surface functional groups of the activated carbon nanospheres. The adsorption kinetic data can be well fitted to the pseudo-second-order kinetics model. The adsorbed silver can be easily recovered by a dilute HNO₃ solution and the carbon nanospheres after silver recovery can be reactivated by the same treatment with NaOH solution. Continuous studies employing a packed column indicated the potential applications of such adsorbents in practical applications for removal of trace amount of Ag(I) ions for drinking water production.

Acknowledgements

This research was funded by Environment and Water Industry Programme Office (EWI) – National Research Foundation Singapore through Project no.: 0802-IRIS-12, and the Ministry of Education, Singapore (grant no.: RG54/05). X.H. Song acknowledges the research scholarship from Nanyang Technological University.

References

- [1] Agency for Toxic Substances Disease Registry (ATSDR), Toxicological Profile for Silver, US Department of Health and Human Services, Atlanta, GA, 1990.
- [2] M.J. Eckelman, T.E. Graedel, Silver emissions and their environmental impacts: a multilevel assessment, *Environ. Sci. Technol.* 41 (2007) 6283–6289.
- [3] M. Hosoba, K. Oshita, R.K. Katarina, T. Takayanagi, M. Oshima, S. Motomizu, Synthesis of novel chitosan resin possessing histidine moiety and its application to the determination of trace silver by ICP-AES coupled with triplet automated-pretreatment system, *Anal. Chim. Acta* 639 (2009) 51–56.
- [4] A. Dabrowski, Adsorption—from theory to practice, *Adv. Colloid Interface Sci.* 93 (2001) 135–224.
- [5] J.M. Dias, M.C.M. Alvim-Ferraz, M.F. Almeida, J. Rivera-Utrilla, M. Sanchez-Polo, Waste materials for activated carbon preparation and its use in aqueous-phase treatment: a review, *J. Environ. Manage.* 85 (2007) 833–846.
- [6] S. Coruh, G. Senel, O.N. Ergun, A comparison of the properties of natural clinoptilolites and their ion-exchange capacities for silver removal, *J. Hazard. Mater.* 180 (2010) 486–492.
- [7] H. Ghassabzadeh, A. Mohadespour, M. Torab-Mostaedi, P. Zaheri, M.G. Maragheh, H. Taheri, Adsorption of Ag, Cu and Hg from aqueous solutions using expanded perlite, *J. Hazard. Mater.* 177 (2010) 950–955.

- [8] X. Sun, Y. Li, Hollow carbonaceous capsules from glucose solution, *J. Colloid Interface Sci.* 291 (2005) 7–12.
- [9] X. Sun, Y. Li, Colloidal carbon spheres and their core/shell structures with noble-metal nanoparticles, *Angew. Chem. Int. Ed.* 43 (2004) 597–601.
- [10] Y. Wan, Y.L. Min, S.H. Yu, Synthesis of silica/carbon-encapsulated core-shell spheres: templates for other unique core-shell structures and applications in *in situ* loading of noble-metal nanoparticles, *Langmuir* 24 (2008) 5024–5028.
- [11] Y. Shin, L.Q. Wang, I.T. Bae, B.W. Arey, G.J. Exarhos, Hydrothermal syntheses of colloidal carbon spheres from cyclodextrins, *J. Phys. Chem. C* 112 (2008) 14236–14240.
- [12] L. Lai, G. Huang, X. Wang, J. Weng, Solvothermal syntheses of hollow carbon microspheres modified with $-NH_2$ and $-OH$ groups in one-step process, *Carbon* 48 (2010) 3145–3156.
- [13] X. Sun, J. Liu, Y. Li, Use of carbonaceous polysaccharide microspheres as templates for fabricating metal oxide hollow spheres, *Chem. Eur. J.* 12 (2006) 2039–2047.
- [14] H. Qian, G. Lin, Y. Zhang, P. Gunawan, R. Xu, A new approach to synthesize uniform metal oxide hollow nanospheres via controlled precipitation, *Nanotechnology* 18 (2007).
- [15] R. Demir-Cakan, N. Baccile, M. Antonietti, M.M. Titirici, Carboxylate-rich carbonaceous materials via one-step hydrothermal carbonization of glucose in the presence of acrylic acid, *Chem. Mater.* 21 (2009) 484–490.
- [16] Y. Ni, L. Jin, L. Zhang, J. Hong, Honeycomb-like Ni@C composite nanostructures: synthesis, properties and applications in the detection of glucose and the removal of heavy-metal ions, *J. Mater. Chem.* 20 (2010) 6430–6436.
- [17] C.Y. Yin, M.K. Aroua, W. Daud, Review of modifications of activated carbon for enhancing contaminant uptakes from aqueous solutions, *Sep. Purif. Technol.* 52 (2007) 403–415.
- [18] A. Demirbas, Agricultural based activated carbons for the removal of dyes from aqueous solutions: a review, *J. Hazard. Mater.* 167 (2009) 1–9.
- [19] L. Wang, R.G. Xing, S. Liu, H.H. Yu, Y.K. Qin, K.C. Li, J.H. Feng, R.F. Li, P.C. Li, Recovery of silver (I) using a thiourea-modified chitosan resin, *J. Hazard. Mater.* 180 (2010) 577–582.
- [20] A.M. El-Menshawly, I.M. Kenawy, A.A. El-Asmy, Modification of chloromethylated polystyrene with 2-mercaptobenzothiazole for application as a new sorbent for preconcentration and determination of Ag^+ from different matrices, *J. Hazard. Mater.* 173 (2010) 523–527.
- [21] A. Afkhami, T. Madrakian, Z. Karimi, A. Amini, Effect of treatment of carbon cloth with sodium hydroxide solution on its adsorption capacity for the adsorption of some cations, *Colloid Surf. A Physicochem. Eng. Asp.* 304 (2007) 36–40.
- [22] M.R. Mostafa, Adsorption of mercury, lead and cadmium ions on modified activated carbons, *Adsorpt. Sci. Technol.* 15 (1997) 551–557.
- [23] C.A. Toles, W.E. Marshall, M.M. Johns, Surface functional groups on acid-activated nutshell carbons, *Carbon* 37 (1999) 1207–1214.
- [24] J.P. Chen, S.N. Wu, Acid/base-treated activated carbons: characterization of functional groups and metal adsorptive properties, *Langmuir* 20 (2004) 2233–2242.
- [25] D. Zhou, L. Zhang, J. Zhou, S. Guo, Development of a fixed-bed column with cellulose/chitin beads to remove heavy-metal ions, *J. Appl. Polymer Sci.* 94 (2004) 684–691.
- [26] D.D. Duong, *Adsorption Analysis: Equilibria and Kinetics*, Imperial College Press, London, 2003.
- [27] I. Novak, P. Sysel, J. Zemek, M. Pirkova, D. Velic, M. Aranyosiova, Florian, V. Pollak, A. Kleinova, F. Lednický, I. Janigova, Surface and adhesion properties of poly(imide-siloxane) block copolymers, *Eur. Polym. J.* 45 (2009) 57–69.
- [28] X.G. Sun, The investigation of chemical structure of coal macerals via transmitted-light FT-IR microspectroscopy, *Spectrochim. Acta A* 62 (2005) 557–564.
- [29] C. Yao, Y. Shin, L.-Q. Wang, C.F. Windisch, W.D. Samuels, B.W. Arey, C. Wang, W.M. Risen, G.J. Exarhos, Hydrothermal dehydration of aqueous fructose solutions in a closed system, *J. Phys. Chem. C* 111 (2007) 15141–15145.
- [30] S. Shin, J. Jang, S.H. Yoon, I. Mochida, A study on the effect of heat treatment on functional groups of pitch based activated carbon fiber using FTIR, *Carbon* 35 (1997) 1739–1743.
- [31] P.E. Fanning, M.A. Vannice, A drifts study of the formation of surface groups on carbon by oxidation, *Carbon* 31 (1993) 721–730.
- [32] I. Atamanenko, A. Kryvoruchko, L. Yurlova, E. Tsapiuk, Study of the $CaSO_4$ deposits in the presence of scale inhibitors, *Desalination* 147 (2002) 257–262.
- [33] X.H. Guan, G.H. Chen, C. Shang, ATR-FTIR, XPS study on the structure of complexes formed upon the adsorption of simple organic acids on aluminum hydroxide, *J. Environ. Sci. China* 19 (2007) 438–443.
- [34] P. Pendleton, S.H. Wu, A. Badalyan, Activated carbon oxygen content influence on water and surfactant adsorption, *J. Colloid Interface Sci.* 246 (2002) 235–240.
- [35] S.F. Wu, K. Yanagisawa, T. Nishizawa, Zeta-potential on carbons and carbides, *Carbon* 39 (2001) 1537–1541.
- [36] H. Sis, M. Birinci, Effect of nonionic and ionic surfactants on zeta potential and dispersion properties of carbon black powders, *Colloid Surf. A Physicochem. Eng. Asp.* 341 (2009) 60–67.
- [37] X.G. Li, H. Feng, M.R. Huang, Redox sorption and recovery of silver ions as silver nanocrystals on poly(aniline-co-5-sulfo-2-anisidine) nanosorbents, *Chem. Eur. J.* 16 (2010) 10113–10123.
- [38] A.A. Atia, Studies on the interaction of mercury(II) and uranyl(II) with modified chitosan resins, *Hydrometallurgy* 80 (2005) 13–22.
- [39] X.G. Li, X.L. Ma, J. Sun, M.R. Huang, Powerful reactive sorption of silver(I) and mercury(II) onto poly(o-phenylenediamine) microparticles, *Langmuir* 25 (2009) 1675–1684.
- [40] X.G. Li, R. Liu, M.R. Huang, Facile synthesis and highly reactive silver ion adsorption of novel microparticles of sulfodiphenylamine and diaminoanthralene copolymers, *Chem. Mater.* 17 (2005) 5411–5419.
- [41] J. Hanzlik, J. Jehlicka, O. Sebek, Z. Weishauptová, V. Machovic, Multi-component adsorption of $Ag(I)$, $Cd(II)$ and $Cu(II)$ by natural carbonaceous materials, *Water Res.* 38 (2004) 2178–2184.
- [42] C. Chen, J.L. Wang, Removal of Pb^{2+} , Ag^+ , Cs^+ and Sr^{2+} from aqueous solution by brewery's waste biomass, *J. Hazard. Mater.* 151 (2008) 65–70.
- [43] I. Langmuir, The constitution and fundamental properties of solids and liquids, *J. Am. Chem. Soc.* 38 (1916) 2221.
- [44] C.C. Luo, Y.H. Zhang, X.W. Zeng, Y.W. Zeng, Y.G. Wang, The role of poly(ethylene glycol) in the formation of silver nanoparticles, *J. Colloid Interface Sci.* 288 (2005) 444–448.
- [45] J.L. Niu, H.L. Zou, J. Zhang, Z.F. Liu, Tracing the chemical oxidation process of single-walled carbon nanotubes by silver nanoparticles, *Acta Phys. Chim. Sin.* 20 (2004) 1–4.
- [46] Z.R. Yue, W. Jiang, L. Wang, H. Toghiani, S.D. Gardner, C.U. Pittman, Adsorption of precious metal ions onto electrochemically oxidized carbon fibers, *Carbon* 37 (1999) 1607–1618.
- [47] P. Gunawan, R. Xu, Direct assembly of anisotropic layered double hydroxide (LDH) nanocrystals on spherical template for fabrication of drug-LDH hollow nanospheres, *Chem. Mater.* 21 (2009) 781–783.
- [48] B. Hai, J. Wu, X. Chen, J.D. Protasiewicz, D.A. Scherson, Metal-ion adsorption on carboxyl-bearing self-assembled monolayers covalently bound to magnetic nanoparticles, *Langmuir* 21 (2005) 3104–3105.
- [49] Y. Jiang, Q. Gao, H. Yu, Y. Chen, F. Deng, Intensively competitive adsorption for heavy metal ions by PAMAM-SBA-15 and EDTA-PAMAM-SBA-15 inorganic-organic hybrid materials, *Micropor. Mesopor. Mater.* 103 (2007) 316–324.
- [50] L. Yang, Y. Li, X. Jin, Z. Ye, X. Ma, L. Wang, Y. Liu, Synthesis and characterization of a series of chelating resins containing amino/imino-carboxyl groups and their adsorption behavior for lead in aqueous phase, *Chem. Eng. J.* 168 (2011) 115–124.